Since January 2020 Elsevier has created a COVID-19 resource centre with free information in English and Mandarin on the novel coronavirus COVID-19. The COVID-19 resource centre is hosted on Elsevier Connect, the company's public news and information website.

Science of the Total Environment 742 (2020) 140556

Contents lists available at ScienceDirect

Science of the Total Environment

journal homepage: www.elsevier.com/locate/scitotenv

Impact of city lockdown on the air quality of COVID-19-hit of Wuhan city

Xinbo Lian [a], Jianping Huang [a,b,*], Rujin Huang [c,**], Chuwei Liu [a], Lina Wang [d], Tinghan Zhang [a]

[a] Collaborative Innovation Center for Western Ecological Safety, Lanzhou University, Lanzhou 730000, China
[b] CAS Center for Excellence in Tibetan Plateau Earth Sciences, Beijing 100101, China
[c] Institute of Earth Environment, Chinese Academy of Sciences, Xian 710061, China
[d] Gansu Province Environmental Monitoring Center, Lanzhou, 730000, China

HIGHLIGHTS

- The AQI of Wuhan City decreased significantly, the higher the population density, the more significant the decline.
- NO_2 decreased most in Wuhan, but O_3 increased significantly, and Hubei Province also had the same trend.
- The mobile source emission ratio and the local pollution contribution in Wuhan decreased.

GRAPHICAL ABSTRACT

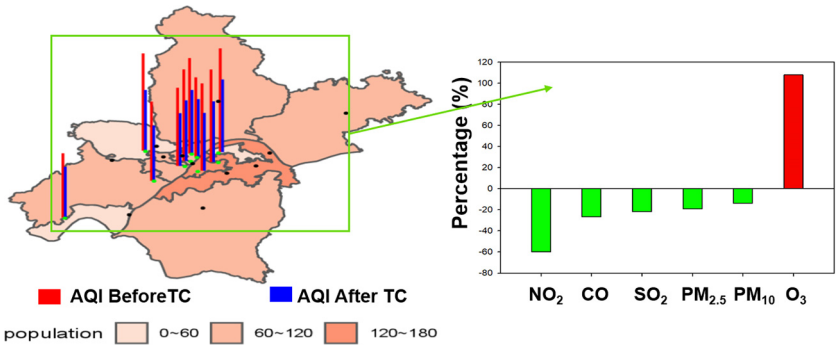

ARTICLE INFO

Article history:
Received 6 May 2020
Received in revised form 24 June 2020
Accepted 25 June 2020
Available online 30 June 2020

Keywords:
COVID-19
Lockdown
AQI
$PM_{2.5}$
NO_2
O_3

ABSTRACT

A series of strict lockdown measures were implemented in the areas of China worst affected by coronavirus disease 19, including Wuhan, to prevent the disease spreading. The lockdown had a substantial environmental impact, because traffic pollution and industrial emissions are important factors affecting air quality and public health in the region. After the lockdown, the average monthly air quality index (AQI) in Wuhan was 59.7, which is 33.9% lower than that before the lockdown (January 23, 2020) and 47.5% lower than that during the corresponding period (113.6) from 2015 to 2019. Compared with the conditions before the lockdown, fine particulate matter ($PM_{2.5}$) decreased by 36.9% and remained the main pollutant. Nitrogen dioxide (NO_2) showed the largest decrease of approximately 53.3%, and ozone (O_3) increased by 116.6%. The proportions of fixed-source emissions and transported external-source emissions in this area increased. After the lockdown, O_3 pollution was highly negatively correlated with the NO_2 concentration, and the radiation increase caused by the $PM_{2.5}$ reduction was not the main reason for the increase in O_3. This indicates that the generation of secondary pollutants is influenced by multiple factors and is not only governed by emission reduction.

1. Introduction

Recently, a new type of coronavirus has caused mass viral pneumonia (COVID-19), thus posing a major threat to international health (Zhou et al., 2020). At present, the epidemic constitutes a public health emergency of international concern (WHO, 2020). Since the middle of December 2019, a number of family clustering outbreaks and transmission from patients to health-care workers have occurred, which shows

* Correspondence to: J. Huang, Collaborative Innovation Center for Western Ecological Safety, Lanzhou University, Lanzhou 730000, China.
** Correspondence to: R. Huang, Institute of Earth Environment, Chinese Academy of Sciences, Xian 710061, China.
E-mail address: hjp@lzu.edu.cn (J. Huang).

https://doi.org/10.1016/j.scitotenv.2020.140556
0048-9697/

that human-to-human transmission has happened through close contact (Huang et al., 2020). Most countries have imposed city lockdown and quarantine measures to reduce transmission to control the epidemic. The Chinese Health Authorities have made considerable efforts, including the positive detection of cases and retrospective investigation of patient clusters. Public risk communication activities have been performed to improve public awareness of self-protection (Hui et al., 2020). The Chinese government has gradually implemented a strict lockdown on Wuhan and surrounding cities as of January 23. Some processing and light industries have been shut down, and the catering and entertainment industries have temporarily closed, and flights, trains and public transport have been suspended (Wu et al., 2020).

In addition to reducing the spread of the disease, the lockdown measures may also have additional health benefits. After the lockdown of city traffic, personnel flow control became the most important aspect. Traffic pollution produces nitrogen monoxide (NO), carbon monoxide (CO), carbon dioxide (CO_2), diesel-exhaust particles, and ozone (O_3), nitrogen dioxide (NO_2), secondary aerosols formed through physical and chemical processes, and pollutants that arise from brake wear, tire wear and re-suspended particles (e.g., trace metals) (Beckerman et al., 2008; Guo et al., 2020). There was a notable association between traffic-related air pollution and premature mortality, and the risk of respiratory and cardiovascular diseases increased in residents living close to high-traffic pollution areas (Brugge and Rioux, 2007; Im et al., 2019). Reducing the emissions from motor vehicles, especially trucks and buses, could produce considerable health benefits (Kheirbek et al., 2016). A survey of hospital visits in Busan city before and after the Asian Games shows that the traffic flow control over 14 consecutive days is associated with a significant decline in the hospitalization rate of children with asthma (Lee et al., 2007). In addition, the reduction in industrial activities after the lockdown also imposes certain environmental and health effects. For example, oil shale mining and power generation processes discharge excessive sulfur dioxide (SO_2), particulate matter (PM_{10}) and nitrogen oxides (NO_x), as well as various other industrial pollutants, such as benzene and phenol, and trace elements (Saurabh Sonwani, 2016).The spatial lag model with fixed effects demonstrates that industrial air pollution causes an increase in medical expenses (Zeng, 2019). Compared to nonindustrial areas, the residents of industrial areas more frequently reported wheezing, chest tightness, shortness of breath, hypertension, heart diseases, etc. (Orru et al., 2018).

Wuhan is the transportation and trade center of Central China, a megacity and national central city of China, with a well-developed transportation system and a large number of motor vehicles. Due to the lack of central heating and chemical industry, in addition to the emissions from coal-fired enterprises such as power plants and the pollution transported from surrounding rural biomass burning activities, vehicle emissions are responsible for the most important pollution source affecting the air quality and public health in Wuhan (Daoru Liu et al., 2020). Wang et al. found that regional traffic has a significant impact on the formation of haze in Wuhan, and the main potential pollution sources are located in the north and south of Wuhan (Si Wang et al., 2017). Liao et al. found that the increase in secondary organics $(NH_4)_2SO_4$ and NH_4NO_3 caused by vehicle exhaust and coal burning as well as the increased environmental moisture absorption were the main causes of pollution in Wuhan (Liao Weijie et al., 2020).

In this report, we studied the change in air quality one month before and after the lockdown in Wuhan and compared it to that during corresponding periods. We analyzed the real-time concentrations of the six air pollutants monitored by the State Control Station, including fine particulate matter ($PM_{2.5}$), PM_{10}, SO_2, NO_2, CO, and O_3, and compared the effects of the lockdown on the concentrations of the different pollutants. We studied the changes in $PM_{2.5}$, NO_2, and O_3 in Hubei Province one month before and after the closure of major cities severely affected by the epidemic and to further analyze the impact of human activities and the lockdown on atmospheric pollutant concentrations.

2. Data and measurement

The daily AQI data of Wuhan, from 1 January 2016 to 31 February 2020, were provided by the Wuhan Ecology and Environment Bureau (http://hbj. wh.gov.cn/). The ground observation daily data of Hubei province were provided by the China National Environmental Monitoring Centre (http://www.cnemc.cn/). Considering the retention of air pollutants, the data from 24 January 2020, to 23 February 2020, are selected as the representative data after the lockdown, and the data from 24 December 2019, to 23 January 2020, are selected as the representative data before the lockdown. The historical data for the sake of comparison during the same period is from 24 January to 23 February 2015–2020, which includes the yearly Chinese Spring Festival holiday. All monitoring instruments of the Wuhan air quality automatic monitoring system operate automatically 24 h a day. The monitoring items are $PM_{2.5}$, PM_{10}, SO_2, NO_2, CO and O_3. The automatic monitoring of $PM_{2.5}$ and PM_{10} adopts the micro-oscillating balance method and the β-absorption method, respectively (ambient air quality standards, GB 3095-2012), and their measuring instruments are a tapered element oscillating microbalance (TEOM) (Rupprecht & Patashnick Co, USA) and a BAM 1020 (Met One Instrument, USA), respectively. SO_2, NO_2, CO and O_3 were measured by instruments of TEI-43i, TEI-42i, TEI-48i and TEI-49i (Thermo Fisher Scientific, USA), respectively. The experimental methods are as follows the ultraviolet fluorescence method (SO_2), the chemiluminescence method (NO_2), the nondispersion infrared absorption method and gas filter correlation infrared absorption method (CO), and the UV-spectrophotometry (O_3).

The average air quality index (AQI) is a dimensionless index, which is calculated according to the Chinese ambient air quality standard (G B3095-2012) and includes six pollutants in the calculation, i.e., SO_2, NO_2, PM_{10}, $PM_{2.5}$, O_3 and CO. The subindex of each pollutant is first calculated according to the fractional concentration and is labeled $IAQI_P$.

$$IAQI_p = \frac{IAQI_{Hi} - IAQI_{L0}}{BP_{Hi} - BP_{L0}}(C_P - BP_{L0}) + IAQI_{L0} \quad (1)$$

In Eq. (1), IAQIp is the air quality subindex of pollutant P; C_P is the mass concentration of pollutant P; BP_{Hi} is the upper limit value of the pollutant concentration close to C_P in Table 1; BP_{Lo} is the lower limit value of the pollutant concentration close to C_P in Table 1; $IAQI_{Hi}$ is the air quality subindex corresponding to BP_{Hi} in Table 1; and $IAQI_{Lo}$ is the air quality subindex corresponding to BP_{Lo} in Table 1. When the AQI is higher than 50, the pollutants with the highest air quality subindex are the primary pollutants. If there are two or more pollutants with the highest air quality subindex, they are listed as the primary pollutants. In addition, the pollutants with an IAQI higher than 100 are overstandard pollutants. A high AQI indicates that serious and concentrated air pollution will not only affect the outdoor activities of humans but also damage their health.

3. Results

3.1. A spatial comparison of AQI before and after lockdown

The main administrative regions of Wuhan are relatively concentrated and the population difference is notable, the population density decreases from the central regions to the peripheral regions (Fig. 1a). After the lockdown, the AQI in the different administrative regions in Wuhan decreased, of which the air quality at Wujiashan station and Qiaokou Gutian station exhibited the most notable improvement (decreasing 37.4% and 37.3%, respectively), while Xinzhou district station attained the smallest decrease of 15.5%. The results show that the AQI improvement rate increased with the increase in population density

Table 1
Pollutant concentration limits.

IAQI	SO_2 (24-h average, μg/m^3)	SO_2 (1-h average, μg/m^3)	NO_2 (24-h average, μg/m^3)	NO_2 (1-h average, μg/m^3)	PM_{10} (24-h average, μg/m^3)	CO (24-h average, mg/m^3)	CO (1-h average, mg/m^3)	O_3 (1-h average, μg/m^3)	O_3 (8-h average, μg/m^3)	$PM_{2.5}$ (24-h average, μg/m^3)
0	0	0	0	0	0	0	0	0	0	0
50	50	150	40	100	50	2	5	160	100	35
100	150	500	80	200	150	4	10	200	160	75
150	475	650	180	700	250	14	35	300	215	115
200	800	800	280	1200	350	24	60	400	265	150
300	1600	/	565	2340	420	36	90	800	800	250
400	2100	/	750	3090	500	48	120	1000	/	350
500	2620	/	940	3840	600	60	150	1200	/	500

(Fig. 1b). The average AQI improvement rate in districts with a population density of less than 5000 was 25.7%, whereas that in areas with a population density of more than 20,000 was 34.9%. This difference was due to the frequent traffic congestion in populated areas before the lockdown, leading to additional emissions of exhaust gas. The wear and tear of roads, tires, and brakes caused by congestion are also sources of particulate matter (Han and Sun, 2019). Furthermore, the high density of buildings reduces the wind speed and the diffusion of air pollution (Liu et al., 2017).

After lockdown, of the nine state-controlled monitoring sites (excluding the background station), Hanyang Yuehu Station had the lowest AQI (54.1) because the site is far from the city's main roads and industrial areas. Qingshan Ganghua Station had the highest AQI (73.2) because it is close to Wuhan iron and steel Corporation. Studies have shown that the contribution rate of $PM_{2.5}$ from steel industry pollution sources in Wuhan in winter is second only to traffic sources, up to 30.8% (Huang et al., 2019). Therefore, the high AQI of the site during the implementation of government intervention measures may be mainly influenced by heavy industry sources.

3.2. A comparison of the AQI from 2020 with that in 2015–2019 for the same period and before the control

We selected the period December 24, 2019 to January 23, 2020 as the period before the lockdown, and compared this period with the historical corresponding periods of January 24 to February 23 from 2015 to 2019. After the lockdown, the average AQI in Wuhan was 59.7, a decrease of 47.5% compared to that during the corresponding period from 2015 to 2019 (Fig. 2a). Compared with before the lockdown, the average AQI decreased by 33.9%, and the differences among monitoring sites also decreased significantly (Fig. 2b). The rate of days with an AQI < 100 was 96.8%, of which 41.9% had an AQI < 50, without moderately and severely polluted days. Compared with the corresponding periods, the rate of good days (AQI < 100) increased by 37.4%, which means that during the lockdown, the air quality in Wuhan had no significant effect on human health, and only some pollutants may have had a weak impact on the health of a small number of unusually sensitive people.

Among the 18 pollution days, $PM_{2.5}$ was the primary pollutant on 16 days (88.9%), PM_{10} and O_3 were the primary pollutants on 1 day

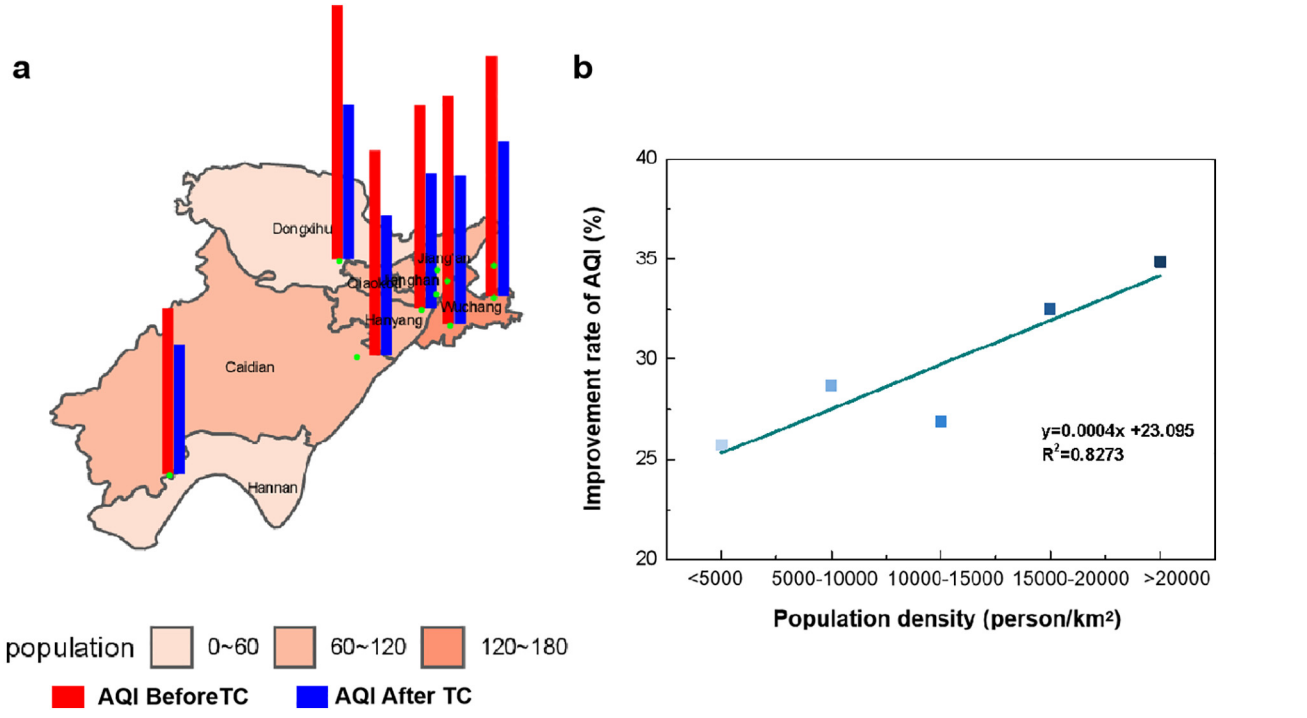

Fig. 1. The geography of Monitoring stations, and the relationship between AQI and population. a, The spatial distribution of AQI and population (10,000 people) in Wuhan, AQI before lockdown (red) and after (blue). b, The relationship between the improvement rate of AQI and population density.

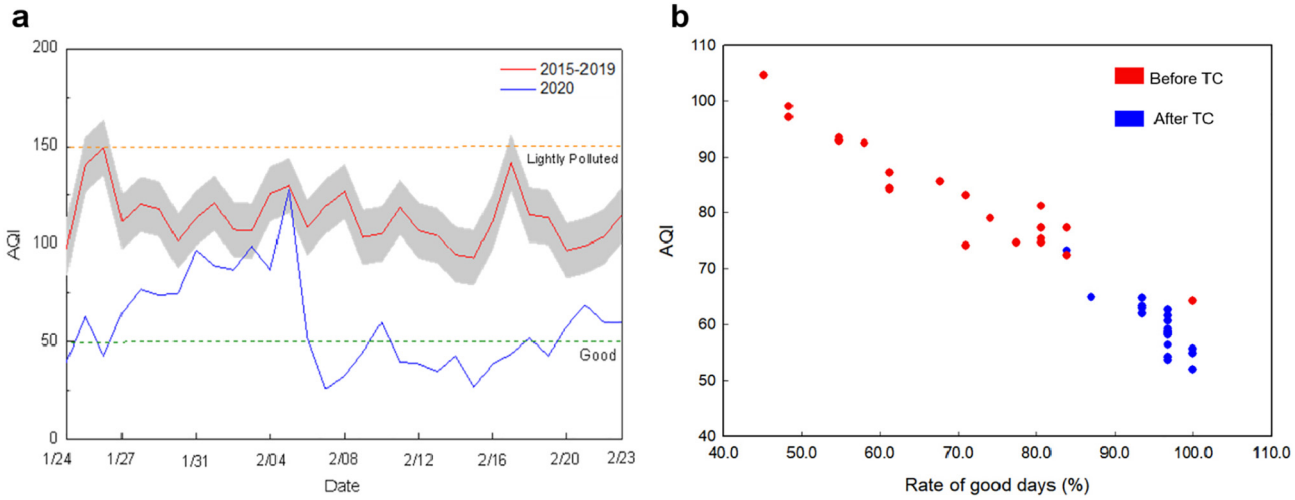

Fig. 2. Time change of AQI in Wuhan after the lockdown. a, AQI after lockdown compared with the historical period from 2015 to 2019. b, The change of AQI and the rate of good days (AQI < 100) at different stations. TC represents the start date of traffic control (January 23, 2020). 1 month before TC is red, 1 month after TC is blue.

(5.6%). On the lightly polluted day (February 5), $PM_{2.5}$ and PM_{10} both increased considerably. Therefore, after the lockdown, the most important influencing factor of the AQI is $PM_{2.5}$ in Wuhan. The proportion of days with an $IAQI_{PM2.5} < 100$ increased substantially, with three stations reaching 100%. This is due to reductions in vehicle emissions and the closure of some industrial plants during government controls, which caused black carbon, organic components, sulphate particulate matter and important precursors such as SO_2, NO_x and hydrocarbons (CH_x) to be reduced to some extent (Richmond-Bryant et al., 2009),(Daellenbach et al., 2016). After the lockdown, the rise of O_3 led to the first polluted day in winter in Wuhan with O_3 as the major pollutant since 2015. There were no days with NO_2 as the main pollutant during the control, which was a significant improvement compared with the historical period from 2015 to 2019 and before the control period.

3.3. The evolution of the pollutant concentration during the lockdown

Compared with the average concentration during the historical 2019 period and before the lockdown, the PM_{10}, $PM_{2.5}$, SO_2, NO_2, and CO concentrations all decreased to some extent, whereas the O_3 concentration increased greatly during the lockdown (Fig. 3). The spatial differences in the pollutant concentrations were small. Due to the reduction in fugitive dust caused by the reduction in vehicles and the stoppage of construction after the lockdown, PM_{10} decreased by 40.2% compared to before the lockdown. The monthly average $PM_{2.5}/PM_{10}$ ratio was 0.9, so $PM_{2.5}$ was the main particle pollutant that decreased by 36.86% (Aldabe et al., 2011). NO_2 exhibited the most notable improvement, with an average concentration reduction of approximately 53.3%, due to NO_2 is highly correlated with traffic pollution. According to the transportation index data, the decrease in national traffic volume

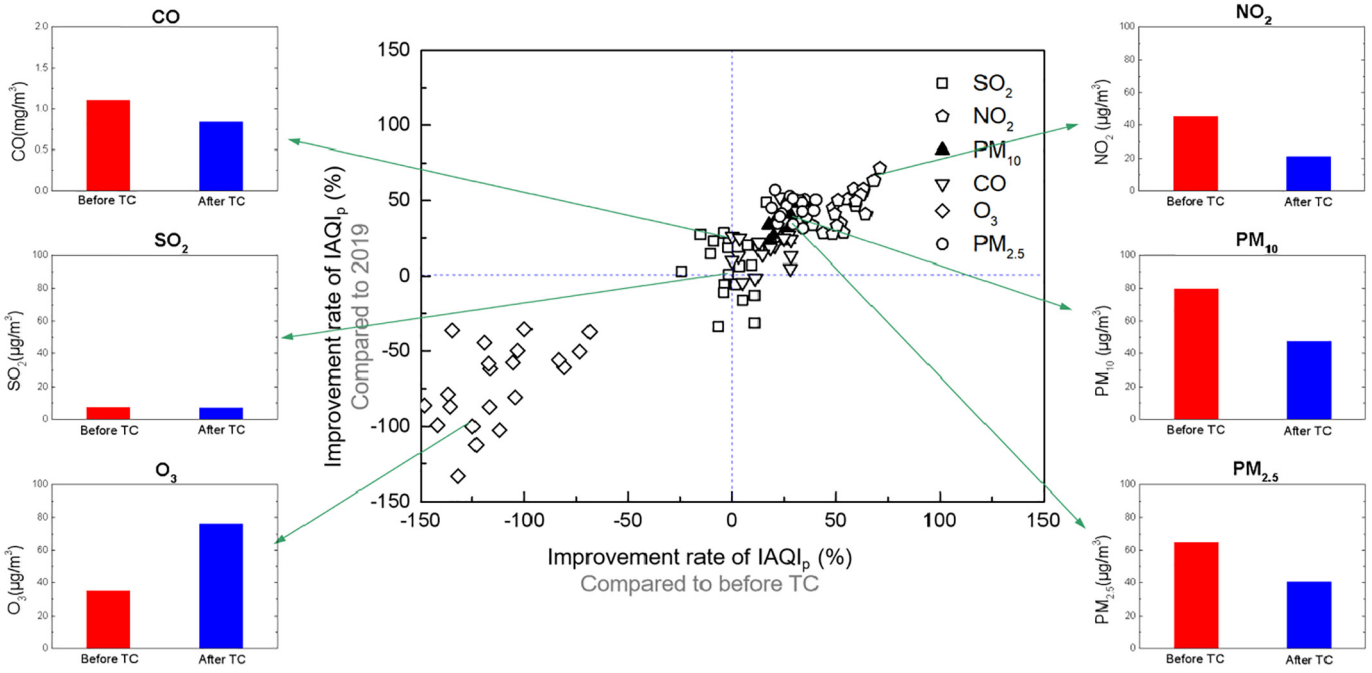

Fig. 3. Improvement rate of pollution factors in Wuhan city after lockdown.

was estimated to be 70% during the lockdown (Xin Huang et al., 2020). O_3 is an important secondary pollutant in warm months but is generally less important in winter. Compared with the conditions before the control measures, the O_3 concentration increased by approximately 116.6%. This may be related to the change in the primary pollutant concentration and meteorological conditions. In addition, O_3 lasts longer in cold weather, which may contribute to its accumulation (Zhang et al., 2016). The smaller decrease in SO_2 of only 3.9% may be related to the increase in domestic heating and cooking during the lockdown period. Compared with the summer of 2019, the SO_2 concentration only increased by approximately 0.6 μg/m^3. This shows that the SO_2 emissions in Wuhan mainly come from power plant emissions and industrial and domestic coal combustion, and the correlations with traffic and heating were low. CO is a product of domestic combustion and power generation. The average CO concentration was 0.9 mg/m^3 (down 22.7%), and the decrease in CO varied greatly among different sites, from 3.2% to 34.5%.

3.4. The diurnal variation in the $PM_{2.5}$, NO_2 and O_3 concentrations

The average daily variation data for 1 month before and after the blockade were selected to analyze $PM_{2.5}$, NO_2, and O_3. Because $PM_{2.5}$ comes from complex sources and the generation of secondary aerosols is affected by a variety of factors, the average daily variation range of $PM_{2.5}$ is small and highly discrete. The daily variation trend in $PM_{2.5}$ after the lockdown was similar to that before, although the range of variation increased and a significant decrease occurred at 18:00, which was attributed to the vertical expansion of the boundary layer and the vertical diffusion of pollutants during the day. (Shi and Brasseur, 2020) (Fig. 4a). The concentration of NO_2 prior to the lockdown showed a peak in the morning and during evening traffic hours (8–11 a.m. and 6–9 p.m., respectively). However, during the lockdown, NO_2 did not exhibit peaks associated with morning rush hours, further indicating that traffic was not a major source of NO_2 during this period (Fig. 4b). Before the lockdown, the diurnal peaks in O_3 occurred at 7:00 and from 15:00. After the lockdown, the range of the daily variation increased considerably. Only the peak from 15:00 was retained and some deviation occurred. In contrast to the control before the lockdown, O_3 showed a downward trend from 00:00 to 10:00, which may be related to the decrease in NO_2 in the peak morning period. When O_3 reached its maximum value, NO_2 and $PM_{2.5}$ decreased to the minimum values. This was probably due to the photolysis consumption of NO_2 and the attenuation of solar radiation caused by the reduction of $PM_{2.5}$ accelerating the formation of O_3 (Ma et al., 2019) (Fig. 4c). In the actual atmosphere, the O_3 concentration is also affected by meteorological elements and important precursors such as volatile organic compounds (VOCs) and CO. When the VOC concentration and NO_x ratio are unbalanced, this will also affect the steady-state cycle (Chung et al., 1996).

3.5. The mass concentration ratios of $[NO_2]/[SO_2]$ and $[CO]/[SO_2]$ during the lockdown

In the atmosphere, $[NO_2]/[SO_2]$ is often adopted to indicate the change in the contribution rates of mobile and fixed emission sources. Studies have reported that the SO_2 emissions from motor vehicles in northern China is far lower than the NOx emissions, and the emission ratio of $[NO_2]/[SO_2]$ from motor vehicles ranged from 24 to 119 (Fiedler et al., 2009). Both NO_x and SO_2 are discharged from stationary sources, with relatively more SO_2. The ratio of $[NO_2]/[SO_2]$ from stationary sources ranged from 0.2 to 0.8 (Fiedler et al., 2009). After the lockdown, $[NO_2]/[SO_2]$ decreased significantly ($P < 0.01$), and the contribution rate of fixed sources increased (factories, power plants, chimneys and boilers, etc.), while the contribution rate of mobile sources decreased, which was consistent with the reduction in vehicle emissions (Fig. 5a) (Ji et al., 2012).

In Wuhan, SO_x is not the main component of air pollutants because the levels of industry, coal pollution, and central heating pollution are low. However, Wuhan is a mega-city with a population of more than 10 million and has a developed transportation system with a large number of motor vehicles. Thus, CO emissions are higher than SO_2 emissions $[CO]/[SO_2]$ can be adopted to roughly evaluate the impact and contribution of local pollutant discharge and external pollutant transportation on the pollution process, with higher ratios indicating higher local contributions (Zhu et al., 2015). After the lockdown, $[CO]/[SO_2]$ decreased significantly ($P < 0.01$) in Wuhan, which indicated that the contribution rate of local emissions decreased, and the air pollution in local areas was affected by surrounding or remote sources (Fig. 5b). The transport pathways in Wuhan were identified to be the northwest, east and south pathways (with relative contribution rates of 40%, 17% and 43%, respectively), and the major potential source regions were western Henan, northern Shanxi and southwestern Shanxi (Huang et al., 2019).

3.6. The air quality improvement in Hubei Province during the lockdown period

As shown in Fig. 6, 12 cities in Hubei Province were selected for analysis. After the lockdown, the average monthly $PM_{2.5}$ concentration in each city ranged from 31.2 μg/m^3 (Xianning) to 64.6 μg/m^3 (Xiangyang). According to the Chinese Ambient Air Quality Standards (CAAQS) (GB3095-2012), the average monthly $IAQI_{PM2.5}$ in Xianning City was 44, thus reaching good level, and the average monthly $IAQI_{PM2.5}$ values in the other 11 cities were moderate. The reason for the high $PM_{2.5}$ concentration in Xiangyang may be that the area has a large population, and the area of cultivated land ranks first in Hubei Province, which generates more agricultural pollution (ammonia-nitrogen fertilizers) (Wu et al., 2016). The improvement rate of NO_2 is substantially higher than other pollutants, with an average concentration range of 8.1 μg/m^3 (Xianning) - 21.4 μg/m^3 (Wuhan) after the lockdown. The average concentration range of O_3 was 73.0 μg/m^3 (Xianning) - 88.2 μg/m^3 (Jingmen), which

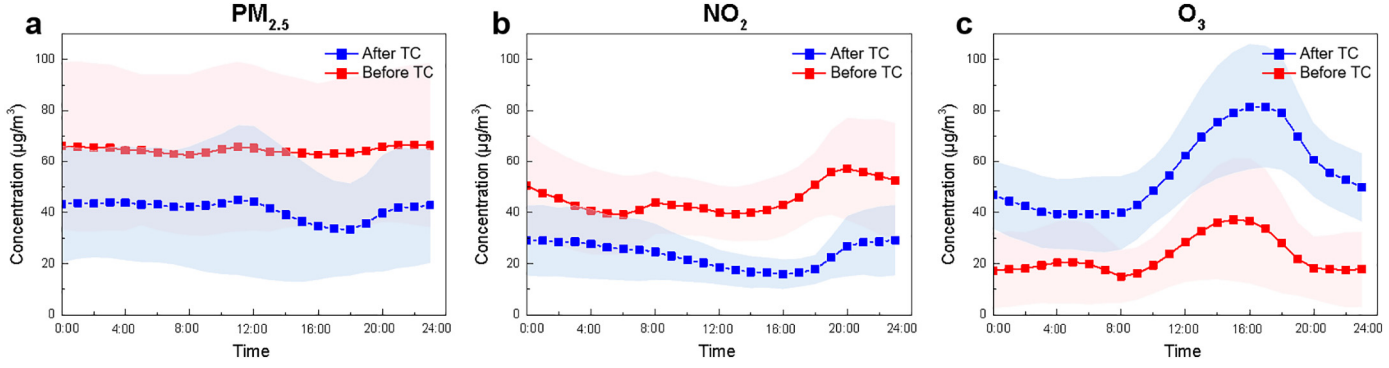

Fig. 4. Diurnal variation of $PM_{2.5}$, NO_2 and O_3 concentrations before and after lockdown. a, $PM_{2.5}$. b, NO_2. c, O_3.

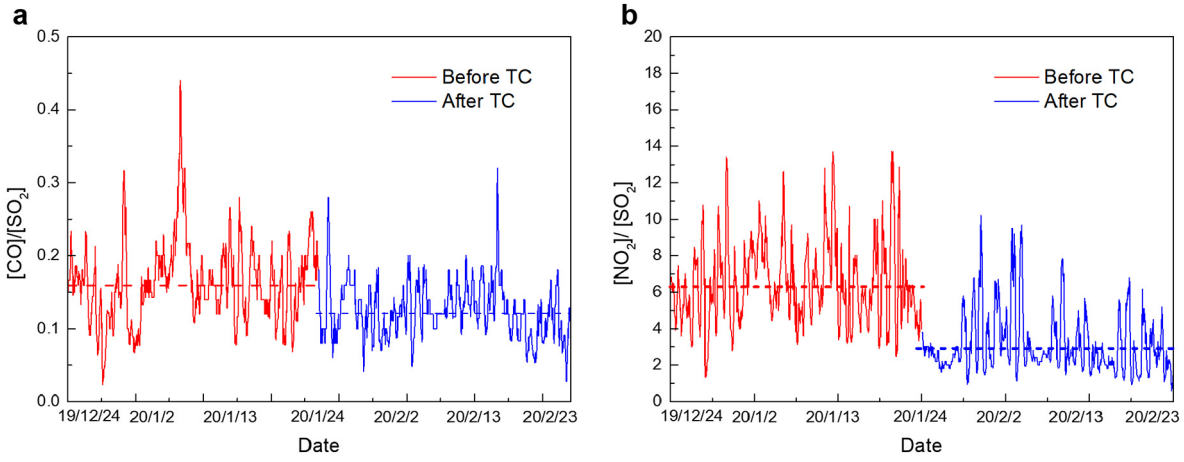

Fig. 5. The change of $[NO_2]/[SO_2]$ and $[CO]/[SO_2]$ after the lockdown. **a**, $[NO_2]/[SO2]$ b, $[CO]/[SO_2]$. The dotted line represents the monthly average before and after the lockdown, with a significant difference ($P < 0.001$).

was much higher than that before the lockdown, and it did not exceed the air quality standards in terms of potentially harming human health. The improvement rates of the AQI and $PM_{2.5}$ are lowest, 23.7% and 28.6%, respectively, when the population density ranged from 400 to 800 person/km^2. The population density of Wuhan reached 1304.6 person/km^2, and the improvement rate was significantly higher than that in the other cities except Yichang and Xianning. The transportation industry in Yichang and Xianning is relatively well developed, and the passenger traffic volume was larger than 50 million in 2018 in Xianning (Statistics., 2020). The restrictions on vehicles during the control period may be the main reasons for the high improvement rate of $PM_{2.5}$ in the two regions.

4. Discussion

CO mainly comes from the incomplete combustion of fossil fuel (the exhaust gas of internal combustion engines, combustion of boiler fuel, etc.) and biomass combustion (combustion of crop straw in open fields). Generally, in winter, automobile exhaust contributes approximately 50% to the CO quality of the lower atmosphere of the city (mostly in the morning and evening hours and very little at night), and the contribution of wood combustion is approximately 30% (mostly in the evening and nighttime and very little during the day) (Khalil and Rasmussen, 1988). After the lockdown, the decline in CO was far lower than 50%, and there was no clear trend of daily CO change, which shows that after the lockdown, the CO emissions from industrial boiler fuel and domestic coal combustion in the Wuhan area account for a large proportion. The main source of gaseous SO_2 is the combustion of sulfur-containing fuels (oil, coal and diesel) (Huang et al., 2012). After the control period, the SO_2 improvement was not distinct. On the one hand, many coal-fired industries were not shut down, mainly due to the effectiveness of pollution control in recent years. Compared to 2015, the SO_2 concentration decreased 20.5 μg/m^3, which is due to the upgrading of key industrial industries (power and steel), especially the role of the ultralow emissions of electric power generation, elimination of small and medium-sized coal-fired boilers, conversion of rural heating from coal to gas and electricity and other policies in recent years.

The drop in $PM_{2.5}$ and PM_{10} after the lockdown was not as major as expected, which may be related to a number of factors. First, after the lockdown, the most intensive control concerned traffic, and traffic pollution is not the most important source of $PM_{2.5}$ in Wuhan (Zong et al., 2020). Second, since the implementation of the national policy on smog governance, the fine particulate emissions in China have been effectively controlled, especially in areas where central heating is generally not provided, such as central and southern China (Wang et al., 2020a, 2020b). Since 2013, the national average annual concentration of $PM_{2.5}$ has dropped substantially, and the number of heavily polluted days has decreased drastically, especially in autumn and winter (Ministry, 2020b). Third, due to the epidemic control period and the return of migrant workers, the proportion of bulk coal heating users has increased, which may also have mitigated some of the reductions in $PM_{2.5}$, NO_x and SO_2 due to the decreased vehicle emissions (Ministry, 2020a). Recently studies have shown that the formation of secondary particles significantly enhanced during the lockdown (Xin Huang et al., 2020). In the early stage, Wuhan coal combustion was the main source of NO_x (41.0% ± 13.7%), and motor vehicle emissions were the second main source (21.8%) from 2013 to 2014 (Zong et al., 2020). After the implementation of emission standards of coal-fired power plants, multiple technical improvements such as SCR, SNCR, etc., greatly decreased the NO_2 emissions from coal-fired sources, which further led to the most notable improvement in NO_2 after the traffic control due to the increasing of the proportion of NO_2 traffic source emissions.

At present, O_3 pollution has occurred in most parts of China in summer and tends to be a complex type of air pollution ($PM_{2.5}$ pollution in winter and O_3 pollution in summer). This study shows that the O_3 concentration may also become a major pollutant in winter, requiring further analysis of the reasons for its rise to avoid more serious O_3 pollution in winter. After the lockdown, the NO_x control effect is very distinct; however, the effectiveness of the VOC control measures needs to be further studied. A change in NO_x to VOC ratio may also lead to an increase in O_3 generation (Owoade et al., 2015). The transformation and connection between pollutants in terms of the quality and quantity are very complicated. Although NO_x is one of the precursors of O_3, NO_x reduction has a negative effect on the O_3 concentration. Therefore, the generation of secondary pollutants is affected by multiple factors, and its governance is not only related to emission reductions.

Meteorological elements play significant roles in air pollution formation, transport, deposition and transformation. The relatively low relative humidity and wind speed in winter are conducive to the generation and resuspension of dust, and the height of the boundary layer is low, while precipitation is low, which is conducive to the accumulation of secondary sulfate and nitrate (Miao et al., 2018). In Wuhan, the formation of O_3 at the urban site is controlled by VOC_s, while the formation of O_3 at the urban site is controlled by VOC_s and NO (Zhu et al., 2020). VOC_s is greatly affected by pollution sources, photochemical reaction processes and regional transportation (Zhu et al., 2020). A recent study by Wang et al. suggested that meteorological conditions in most Chinese cities caused an increase in pollutants that outweighed the positive impact of emission reductions during COVID-19 outbreak, but for Wuhan, unfavorable meteorology had less effect compared with emission changes (Wang et al., 2020a, 2020b). However, the reason for the

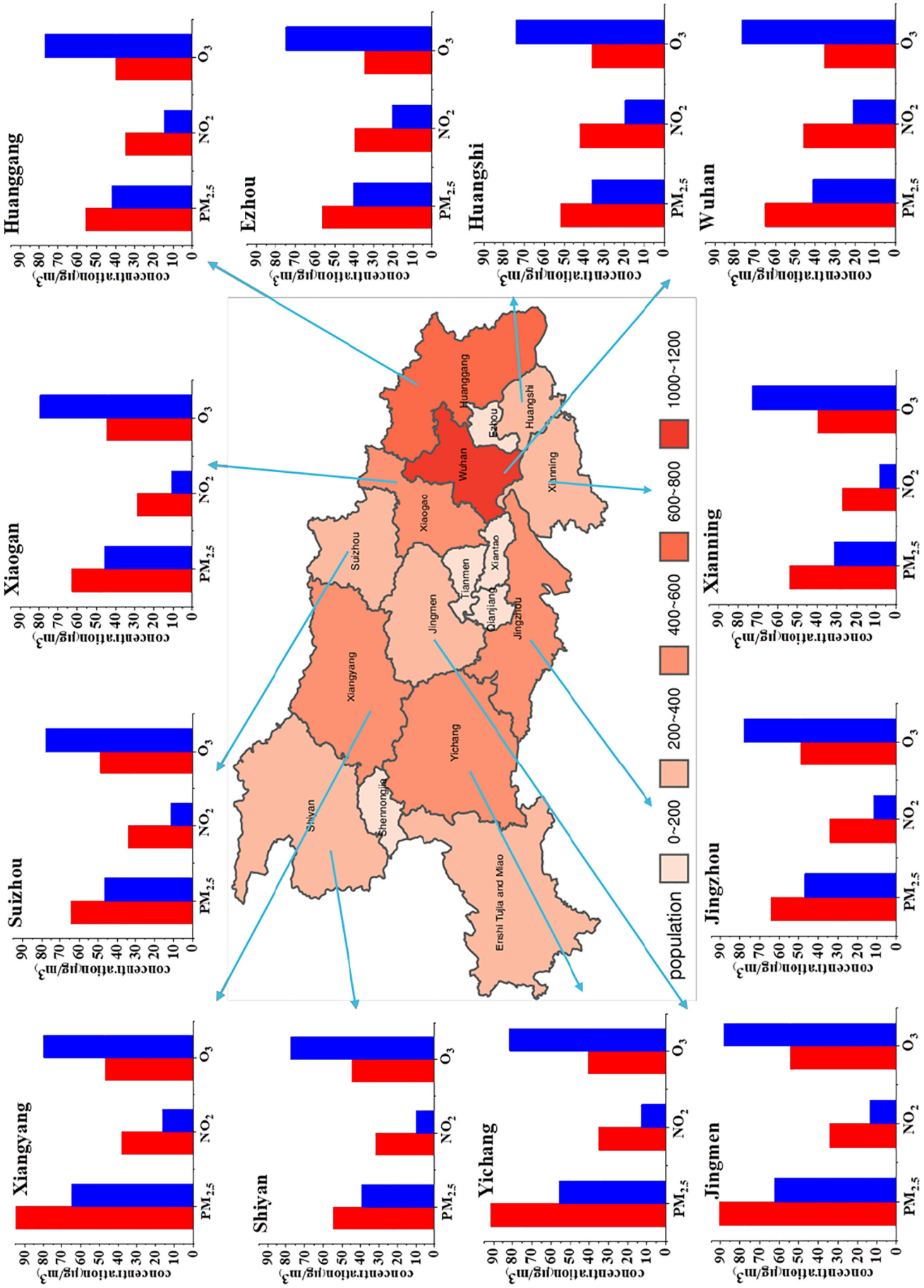

Fig. 6. The spatial distribution of geotagged cities $PM_{2.5}$, NO_2, O_3 concentration and population (10,000 people) in Hubei. Before lockdown (red), after lockdown (blue).

increase in O_3 needs to be combined with meteorological conditions of photochemical production for further research.

5. Conclusion

Our results show that the air quality in Hubei province and Wuhan improved significantly during the COVID-19 lockdown, with concentrations of all six standard pollutants, except O_3, dropping to some extent with the largest decrease in NO_2. The significant increase in the O_3 concentration may be related to the changes in NO_2, VOC_s, and $PM_{2.5}$, and the reaction mechanism should be studied further in combination with meteorological elements and the photochemical mechanism. Air pollution is a complex problem linked to multiple factors. The reduction in pollutant discharge will improve air quality, but it may also bring new problems. The generation mechanism of secondary pollutants should be investigated to provide a more comprehensive scientific basis for formulating pollution prevention and control policies.

Graphics software

All maps and plots were produced using licensed.

CRediT authorship contribution statement

Xinbo Lian: Formal analysis, Data curation, Writing - original draft, Writing - review & editing.**Jianping Huang:**Conceptualization, Data curation, Writing - original draft, Writing - review & editing.**Rujin Huang:**Conceptualization, Data curation, Writing - original draft, Writing - review & editing.**Chuwei Liu:**Formal analysis, Data curation, Writing - original draft, Writing - review & editing.**Lina Wang:**Formal analysis, Data curation, Writing - original draft, Writing - review & editing.**Tinghan Zhang:**Formal analysis, Data curation, Writing - original draft, Writing - review & editing.

Declaration of competing interest

The authors declare that they have no known competing financial interests or personal relationships that could have appeared to influence the work reported in this paper.

Acknowledgements

This work was jointly supported by the National Natural Science Foundation of China (41521004) and the Gansu Provincial Special Fund Project for Guiding Scientific and Technological Innovation and Development (Grant No. 2019ZX-06). The authors acknowledge the Wuhan bureau of ecology and environment for providing the datasets. http://hbj.wuhan.gov.cn/.

References

Aldabe, J., Elustondo, D., Santamaría, C., Lasheras, E., Pandolfi, M., Alastuey, A., Querol, X., Santamaría, J.M., 2011. Chemical characterisation and source apportionment of $PM_{2.5}$ and PM_{10} at rural, urban and traffic sites in Navarra (north of Spain). Atmos. Res. 102, 0–205.

Beckerman, B.J., Brook, Michael, Verma, Jeffrey R., Arain, Dave K., Finkelstein, Muhammad A., Murray, M., 2008. Correlation of nitrogen dioxide with other traffic pollutants near a major expressway. Atmospheric Environ 42, 275–290.

Brugge, D.D., Rioux, John L., 2007. Christine. Near-highway pollutants in motor vehicle exhaust: a review of epidemiologic evidence of cardiac and pulmonary health risks. Environ. Health 6.

Chung, J., Wadden, Richard A., Scheff, Peter A., 1996. Development of ozone-precursor relationships using VOC receptor modeling. Atmos. Environ. 30, 0–3179.

Daellenbach, K.R., Bozzetti, C., Křepelová, A., Canonaco, F., Wolf, R., Zotter, P., Fermo, P., Crippa, M., Slowik, J.G., Sosedova, Y., 2016. Characterization and source apportionment of organic aerosol using offline aerosol mass spectrometry. Atmos Meas Tech 9, 23–39.

Daoru Liu, Q.D., Ren, Zhigang, Zhou, Zeng, Song, Zhe, Huang, Jiahui, Hu, Ruibo, 2020. Variation trends and principal component analysis of nitrogen oxide emissions from motor vehicles in Wuhan City from 2012 to 2017. Sci. Total Environ. 704.

Fiedler, V., Nau, R., Ludmann, S., Arnold, F., Stohl, A., 2009. East Asian SO_2 pollution plume over Europe – part 1: airborne trace gas measurements and source identification by particle dispersion model simulations. Atmos. Chem. Phys. 9, 4717–4728.

Guo, S.H., Peng, Min, Jianfei, Wu, Zamora, Zhijun, Shang, Misti L., Du, Dongjie, Zheng, Zhuofei, Fang, Jing, Tang, Xin, Rongzhi, Wu, Zeng, Yusheng, Shuai, Limin, Zhang, Shijin, Wang, Wenbin, Ji, Yuan, Li, Yuemeng, Zhang, Yixin, Wang, Annie L., Zhang, Weigang, Zhao, Fang, Gong, Jiayun, Wang, Xiaoli, Molina, Chunyu, Zhang, Mario J., Renyi, 2020. Remarkable nucleation and growth of ultrafine particles from vehicular exhaust. Proc. Natl. Acad. Sci. U. S. A. 117, 3427–3432.

Han, S., Sun, Bindong, 2019. Impact of population density on $PM_{2.5}$ concentrations: a case study in Shanghai. China. Sustainability 11.

Huang, Q., Cheng, S., Perozzi, R.E., 2012. Use of a MM5–CAMx–PSAT modeling system to study SO_2 Source apportionment in the Beijing metropolitan region. Environ. Model. Assess. 17, 527–538.

Huang, F., Zhou, Jiabin, Chen, Nan, Li, Yuhua, Wu, 2019. Shuiping chemical characteristics and source apportionment of $PM_{2.5}$ in Wuhan, China. J. Atmos. Chem. 76, 245–262.

Huang, C., Wang, Y., Li, X., Ren, L., Zhao, J., Hu, Y., et al., 2020. Clinical features of patients infected with 2019 novel coronavirus in Wuhan, China. Lancet (London, England) 395, 497–506.

Hui, D.S.I.A., Madani, Esam, Ntoumi, Tariq A., Kock, Francine, Dar, Richard, Ippolito, Osman, McHugh, Giuseppe, Memish, Timothy D., Drosten, Ziad A., Zumla, Christian, Petersen, Alimuddin, 2020. Eskild. The continuing 2019-nCoV epidemic threat of novel coronaviruses to global health - the latest 2019 novel coronavirus outbreak in Wuhan, China. International journal of infectious diseases : IJID : official publication of the International Society for Infectious Diseases 91, 264–266.

Im, U.C., Nielsen, Jesper H., Sand, Ole-Kenneth, Makkonen, Maria, Geels, Risto, Anderson, Camilla, Kukkonen, Camilla, Lopez-Aparicio, Jaakko, Brandt, Susana, Jorgen, 2019. Contributions of Nordic anthropogenic emissions on air pollution and premature mortality over the Nordic region and the Arctic. Atmos. Chem. Phys. 19, 12975–12992.

Ji, D., Wang, Yuesi, Wang, Lili, Chen, Liangfu, Liu, Zirui, 2012. Analysis of heavy pollution episodes in selected cities of northern China. Atmos. Environ. 50, 338–348.

Khalil, M.A.K., Rasmussen, R.A., 1988. Carbon monoxide in an urban environment: application of a receptor model for source apportionment. Japca 38, 901–906.

Kheirbek, I.H., Douglas, Jay, Ito, Sharon, Matte Thomas, Kazuhiko, 2016. The contribution of motor vehicle emissions to ambient fine particulate matter public health impacts in New York City: a health burden assessment. Environ. Health 15.

Lee, J.-T.S., Ji-Young, Cho, Yong-Sung, 2007. Benefits of mitigated ambient air quality due to transportation control on childhood asthma hospitalization during the 2002 summer Asian games in Busan, Korea. J. Air Waste Manage. Assoc. 57, 968–973.

Liao Weijie, Z.J., Shengjie, Zhu, Anshan, Xiao, Li, Kuan, Schauer James, J., 2020. Characterization of aerosol chemical composition and the reconstruction of light extinction coefficients during winter in Wuhan, China. Chemosphere 241, 125033.

Liu, H., Fang, Chuanglin, Zhang, Xiaoling, Wang, Zheye, Bao, Chao, Li, Fangzheng, 2017. The effect of natural and anthropogenic factors on haze pollution in Chinese cities: a spatial econometrics approach. J. Clean. Prod. 165, 323–333.

Ma, T., Duan, Fengkui, He, Kebin, Qin, Yu, Tong, Dan, Geng, Guannan, Liu, Xuyan, Li, Hui, Yang, Shuo, Ye, Siqi, 2019. Air pollution characteristics and their relationship with emissions and meteorology in the Yangtze River Delta region during 2014–2016. J. Environ. Sci. 83, 8–20.

Miao, Y., Liu, Shuhua, Guo, Jianping, Yan, Yan, Huang, Shunxiang, Zhang, Gen, Zhang, Yong, Lou, Mengyun, 2018. Impacts of meteorological conditions on wintertime $PM_{2.5}$ pollution in Taiyuan, North China. Environ. Sci. Pollut. R 25, 21855–21866.

Ministry of Ecology and Environment of the People's Republic of China, 2020a. Civil Coal Treatment is Still the Key Direction of the Beijing-Tianjin-Hebei Region and its Surrounding Areas.

Ministry of Ecology and Environment of the People's Republic of China, 2020b. Regional Air Quality Has Improved Significantly, but Air Pollution Control Still Has a Long Way to Go.

Orru, H.I., Pindus, Jane, Orru, Mihkel, Kesanurm, Kati, Lang, Kaisa, Tomasova, Aavo, Jelena, 2018. Residents' self-reported health effects and annoyance in relation to air pollution exposure in an industrial area in eastern-Estonia. Inter J Env Res Pub Heal 15.

Owoade, K.O., Hopke, Philip K., Olise, Felix S., Ogundele, Lasun T., Fawole, Olusegun G., Olaniyi, Bamidele H., Jegede, Olugbemiga O., Ayoola, Muritala A., Bashiru, Muniru I., 2015. Chemical compositions and source identification of particulate matter ($PM_{2.5}$ and $PM_{2.5\text{-}10}$) from a scrap iron and steel smelting industry along the Ife–Ibadan highway, Nigeria. Atmos Pollut Res 6, 107–119.

Richmond-Bryant, J., Saganich, C., Bukiewicz, L., Kalin, R., 2009. Associations of $PM_{2.5}$ and black carbon concentrations with traffic, idling, background pollution, and meteorology during school dismissals. Sci. Total Environ. 407, 3357–3364.

Saurabh Sonwani, P.S., 2016. Identifying the sources of primary air pollutants and their impact on environmental health: a review. Int J Eng Tech Res 6, 2454–4698.

Shi, X., Brasseur, Guy P., 2020. The response in air quality to the reduction of Chinese economic activities during the COVID-19 outbreak. Geophys. Res. Lett. 47, e2020GL088070.

Si Wang, S.Y., Yan, Renchang, Zhang, Qingyu, Li, Pengfei, Wang, Liqiang, Liu, Weiping, Zheng, Xianjue, 2017. Characteristics and origins of air pollutants in Wuhan, China, based on observations and hybrid receptor models. J. Air Waste Manage. Assoc. 67, 739–753.

Statistics, 2020. HPBo. Statistical yearbook of Hubei province in 2019. http://tjj.hubei.gov.cn/tjsj/sjkscx/tjnj/qstjnj/.

Tang, G., Zhu, X., Hu, B., Xin, J., Wang, L., Münkel, C., Mao, G., Wang, Y., 2015. Impact of emission controls on air quality in Beijing during APEC 2014: lidar ceilometer observations. Atmos. Chem. Phys. 15, 12667–12680.

Wang, P., Chen, K., Zhu, S., Wang, P., Zhang, H., 2020a. Severe air pollution events not avoided by reduced anthropogenic activities during COVID-19 outbreak. Resour Conserv Recy 158, 104814.

Wang, P., Chen, Kaiyu., Zhu, Shengqiang., Wang, Peng., Zhang, Hongliang, 2020b. Severe air pollution events not avoided by reduced anthropogenic activities during COVID-19 outbreak. Resour Conserv Recy 158.

WHO, 2020. Statement on the Second Meeting of the International Health Regulations (2005) Emergency Committee Regarding the Outbreak of Novel Coronavirus (2019-nCoV).

Wu, Y., Gu, Baojing, Erisman, Jan Willem, Reis, Stefan, Fang, Yuanyuan, Lu, Xuehe, Zhang, Xiuming, 2016. $PM_{2.5}$ pollution is substantially affected by ammonia emissions in China. a 218, 86–94.

Wu, J.T.L., Leung, Kathy, Gabriel, M., 2020. Nowcasting and forecasting the potential domestic and international spread of the 2019-nCoV outbreak originating in Wuhan, China: a modelling study. Lancet 395, 689–697.

Xin Huang, A.D., Gao, Jian, Bo, Zheng, Zhou, Derong, Qi, Ximeng, RongTang, Chuanhua Ren, Nie, Wei, Chi, Xuguang, Wang, Jiaping, Zheng, Xu, LiangduoChen, Yuanyuan Li, Che, Fei, Pang, Nini, Wang, Haikun, Tong, Dan, Qin, Wei, WeiCheng, Weijing Liu, Qinyan, Fu, Chai, Fahe, Davis, Steven J., Zhang, Qiang, He, Kebin, 2020. Enhanced Secondary Pollution Offset Reduction of Primary Emissions during COVID-19 Lockdown in China.

Zeng, J.H., 2019. Qiuqin. Does industrial air pollution drive health care expenditures? Spatial evidence from China. J. Clean. Prod. 218, 400–408.

Zhang, L., Wang, T., Zhang, Q., Zheng, J., Xu, Z., Lv, M., 2016. Potential sources of nitrous acid (HONO) and their impacts on ozone: a WRF-Chem study in a polluted subtropical region. J. Geophys. Res. Atmos. 121.

Zhou, P., Yang, X.-L., Wang, X.-G., Hu, B., Zhang, L., Zhang, W., et al., 2020. A pneumonia outbreak associated with a new coronavirus of probable bat origin. Nature 579, 270–273.

Zhu, J., Cheng, H., Peng, J., Zeng, P., Wang, Z., Lyu, X., et al., 2020. O_3 photochemistry on O_3 episode days and non-O_3 episode days in Wuhan, Central China. Atmos. Environ. 223, 117236.

Zong, Z., Tan, Yang, Wang, Xiao, Tian, Chongguo, Li, Jun, Fang, Yunting, Chen, Yingjun, Cui, Song, Zhang, Gan, 2020. Dual-modelling-based source apportionment of NO_x in five Chinese megacities: providing the isotopic footprint from 2013 to 2014. Environ. Inter. 137, 105592.